Clinical Biochemistry 135 (2025) 110861

Contents lists available at ScienceDirect

Clinical Biochemistry

journal homepage: www.elsevier.com/locate/clinbiochem

Exploratory study of extracellular matrix biomarkers for non-invasive liver fibrosis staging: A machine learning approach with XGBoost and explainable AI

Valeria Carnazzo [a], Stefano Pignalosa [a], Marzia Tagliaferro [a], Laura Gragnani [b], Anna Linda Zignego [c], Cosimo Racco [a], Luigi Di Biase [a], Valerio Basile [d], Gian Ludovico Rapaccini [e], Riccardo Di Santo [f,g], Benedetta Niccolini [f], Mariapaola Marino [e,h,*], Marco De Spirito [e,f], Guido Gigante [i], Gabriele Ciasca [e,f,1,*], Umberto Basile [a,1]

[a] Dipartimento di Patologia Clinica, Ospedale Santa Maria Goretti, A.U.S.L. Latina, 04100 Latina, Italy
[b] Department of Translational Research and New Technologies in Medicine and Surgery, University of Pisa, 56126 Pisa, Italy
[c] Center for Systemic Manifestations of Hepatitis Viruses (MaSVE), Department of Experimental and Clinical Medicine, University of Florence, 50121 Florence, Italy
[d] Clinical Pathology Unit and Cancer Biobank, Department of Research and Advanced Technologies, I.R.C.C.S. Regina Elena National Cancer Institute, 00144 Rome, Italy
[e] Fondazione Policlinico Universitario Agostino Gemelli I.R.C.C.S., 00168 Rome, Italy
[f] Dipartimento di Neuroscienze, Sezione di Fisica, Università Cattolica del Sacro Cuore, 00168 Rome, Italy
[g] Dipartimento di Scienze della Vita, della salute e delle Professioni sanitarie, Link Campus University, Rome, Italy
[h] Dipartimento di Medicina e Chirurgia Traslazionale, Università Cattolica del Sacro Cuore, Rome, Italy
[i] National Center for Radiation Protection and Computational Physics, Istituto Superiore di Sanità, 00161 Rome, Italy

ARTICLE INFO

Keywords:
Biomarkers
ECM
Liver fibrosis
HCV
Collagen-IV
Collagen-III N-peptide
Machine learning
XGBoost
Explainable AI

ABSTRACT

Background: Novel circulating markers for the non-invasive staging of chronic liver disease (CLD) are in high demand. Although underutilized, extracellular matrix (ECM) components offer significant diagnostic potential. This study evaluates ECM-related markers in hepatitis C virus (HCV)-positive patients across varying fibrosis stages.

Methods: Sixty-eight patients with mild-to-moderate fibrosis (F1-F2), sixty-six with advanced fibrosis (F3-F4), and thirty healthy donors were recruited. Inclusion criteria were detectable HCV-RNA and no other liver diseases or co-infections. Levels of ECM markers—hyaluronic acid (HA), laminin (LN), collagen-III N-peptide (PIIIP N-P), collagen-IV (C-IV)—along with cholylglycine (CG) and Golgi protein-73 (GP73), were measured in serum using the MAGLUMI 800 CLIA platform.

Results: Levels of LN, HA, C-IV, PIIIP N-P ($p < 0.001$), and GP73 ($p < 0.01$) increased from controls to F1-F2 and F3-F4. CG levels were higher in pathological subjects compared to controls ($p < 0.001$), but no significant differences emerged between fibrosis stages. These trends persisted after adjusting for age and sex. A multivariate ordinal regression identified LN, PIIIP N-P, and C-IV as promising markers, with an accuracy of 0.77. An XGBoost model improved accuracy to 0.87 and enhanced other metrics. SHAP analysis confirmed these variables as key contributors to the model's predictions.

Conclusion: This study underscores the potential of ECM biomarkers, particularly LN, PIIIP N-P, and C-IV, in non-invasively staging CLD. Furthermore, our preliminary data suggest that a machine learning approach, combined with explainable AI, could further enhance diagnostic accuracy, potentially reducing the need for invasive biopsies.

* Corresponding authors.
E-mail addresses: mariapaola.marino@unicatt.it (M. Marino), gabriele.ciasca@unicatt.it (G. Ciasca).
[1] These authors share the senior authorship.

https://doi.org/10.1016/j.clinbiochem.2024.110861
Received 12 June 2024; Received in revised form 28 November 2024; Accepted 30 November 2024
Available online 13 December 2024

1. Introduction

Chronic liver diseases (CLD) represent a global health problem. It is known that chronic inflammation of the liver leads to the formation of fibrotic tissue and in more severe cases to cirrhosis, finally leading to the development of hepatocellular carcinoma (HCC) [1,2].

Hepatic fibrosis results from several triggers such as chronic infection caused by hepatotropic viruses (hepatitis B virus [HBV] and hepatitis C virus [HCV]), excessive alcohol consumption (alcoholic liver disease [ALD]), non-alcoholic fatty liver disease (NAFLD) and autoimmune liver diseases [3].

Liver fibrogenesis is a dynamic state in which molecular, cellular and tissue processes are highly integrated. Under conditions of chronic liver injury, the profibrogenic environment leads hepatic stellate cells (HSC) to become myofibroblasts like cells (HSC/MFs) through a process of activation and *trans*-differentiation. HSC/MFs abundantly synthesize extracellular matrix (ECM) components, particularly fibrillar collagens, which are known as the main substrates in liver fibrosis [4,5].

Scar tissue physically replaces liver cells but is not able to replace liver function. Additionally, fibrosis can deform the internal liver structure and interfere with hepatic blood flow, limiting blood supply to hepatocytes. In this condition, the liver cells die, resulting in the formation of further scar tissue [6,7]. In some cases, fibrosis can be reversible but, unfortunately, a significant percentage of patients with CLD remain asymptomatic and the diagnosis is delayed, thus bringing the fibrosis to a more severe stage. Indeed, hepatic cirrhosis can be prevented by detection of liver fibrosis at an early stage and before the beginning of clinical symptoms.

Liver biopsy has long represented the "gold standard" to determine the stage of liver fibrosis. In recent years, however, attention has been paid to its limits. It is, in fact, an invasive and painful procedure that requires hospitalization of the patient. Furthermore, the liver biopsy presents some limitations such as sampling error and interpretation variability [8]. Blood tests are included in clinical protocols and combine common available tests (aspartate aminotransferase [AST], alanine aminotransferase [ALT], platelet count, albumin, international normalized ratio [INR]) with demographic data and clinical information.

Furthermore, several commercial panels that combine both indirect and direct markers of liver function have been developed to improve the diagnosis and staging of liver fibrosis [9–11]. The introduction of these biomarkers could enable earlier treatment of patients by providing more accurate assessments of fibrosis severity [12–14]. These models and panels are mostly used to distinguish between two levels of fibrosis: absent-minimal versus moderate-severe; they are not reliable in differentiating between moderate and severe degrees of fibrosis [9].

Given the key role of ECM components in liver fibrosis, we have focused our attention on hyaluronic acid (HA), laminin (LN), collagen type III N-peptide (PIIIP N-P), and type IV collagen (C-IV), as well as other non-ECM emerging markers such as cholylglycine (CG) and Golgi protein-73 (GP73). Along with these markers, we also considered conventional markers of liver injury.

In particular, it is known that HA is increased by the activation of HSC cells and high serum HA levels have a positive correlation with the stage of liver fibrosis in patients with different etiologies of CLD [15,16]. LN is a non-collagenous glycoprotein which is synthesized by HSC and deposited in the hepatic basement membrane. In a healthy liver, LN is found around the vessels, while in a liver with cirrhosis LN deposition appears in other areas. Consequently, increased serum LN levels could be an indicator of chronic liver injury with changes in the liver parenchyma [17]. PIIIP N-P represents the largest ECM components in the liver. Crucially, this marker increases in serum of patients with liver fibrosis, but it is not liver specific, in fact its presence also increases in other pathologies such as lung fibrosis, rheumatoid diseases, and chronic pancreatitis [18,19]. C-IV is a basement membrane component and reflects its regeneration [20–22]. The least studied molecule is CG, the most abundant form of bile acids in serum. Its increase is related to the presence of a hepatic pathology [23]. Expression of GP73 transmembrane protein expressed in epithelial cells, in acute, chronic liver diseases and HCC, is remarkably increased in hepatocytes [24].

All these molecules, given current knowledge, have the potential to serve as biomarkers for hepatic fibrosis. However, they are still underutilized in routine clinical practice. The aim of this study is to measure these markers in HCV-positive patients at different stages of fibrosis and evaluate their potential as a biomarker panel for the non-invasive staging of liver disease. Additionally, we explore the use of machine learning and explainable artificial intelligence (AI) to refine and enhance the performance of this potential biomarker panel.

2. Material and methods

2.1. Patients and methods

One hundred thirty-four patients with HCV infection were enrolled at the MaSVE Center (Center for Systemic Manifestations of Hepatitis Viruses), an outpatient clinic at the University of Florence (Florence, Italy). The stage of liver disease in HCV patients was assessed using liver elastography performed with FibroScan (Echosens, Paris, France), and the resulting liver stiffness values were converted to corresponding METAVIR scores. The inclusion criteria for HCV patients included detectable HCV RNA, a period of at least 6 months free from antiviral therapy, and the absence of co-infection with HIV or HBV. Exclusion criteria included the presence of other forms of liver disease, as indicated by abnormal ceruloplasmin and alpha-1-antitrypsin levels, evidence of autoimmune disorders, plasma cell dyscrasias, or neoplastic pathologies.

For the healthy donor group (30 subjects), inclusion criteria required individuals to be adults between 18 and 70 years old, with no history of liver disease or any other chronic conditions such as diabetes or cardiovascular diseases. Donors were confirmed to have normal liver function through clinical and laboratory evaluations, including normal levels of liver enzymes (ALT, AST), bilirubin, and albumin. Participants were also required to be negative for chronic infections, specifically HBV, HCV, and HIV, and to have no history of excessive alcohol consumption. Additionally, they were non-smokers or occasional smokers, with a body mass index (BMI) within the normal range (18.5 to 25).

2.2. Laboratory investigation

Since biomarker detection requires careful handling starting from the pre-analytical phase, blood samples were collected and stored following a strict protocol. Blood was drawn using standard equipment into anticoagulant-free tubes. The samples were centrifuged at 2500 g for 10 min, then divided into aliquots and stored at −80°C until analysis. Specimens were thawed only once and immediately assayed in a blinded manner, within a single batch, to minimize variability.

Biomarker quantification from the serum of both patients and controls was performed according to a previously established method, ensuring consistency and accuracy throughout the process. The quantification of biomarkers from the serum of both patients and controls followed previously established methods.

Analysis was performed on MAGLUMI 800 CLIA Chemiluminescence Immunoassay (CLIA) System (Shenzhen New Industries Biomedical Engineering Co. Snibe Diagnostics, Shenzhen, China), using the commercially available MAGLUMI kits for HA, LN, PIIIP N-P, C-IV, CG and GP73 according to the manufacturer's protocol. The system employs the ABEI procedure, a non-enzyme small molecule with a proprietary formulation designed to enhance stability in both acidic and alkaline buffers. Using the chemiluminescence method, ABEI reacts with sodium hydroxide (NaOH) and hydrogen peroxide (H_2O_2), producing measurable signals that correspond to different analyte concentrations.

2.3. Data visualization and statistical analysis

Data visualization and statistical analysis were conducted using R (version 4.2.1), OriginPro 2022, and Stata 18.0. Discrete variables are reported as absolute frequencies and percentages. Continuous variables were assessed for normality using the Shapiro-Wilk test and QQ plots, revealing non-normal distributions for some variables. Consequently, continuous variables are described as medians with interquartile ranges (IQR, Q3-Q1). The R package "gtsummary" was employed for tabular data presentation [25]. Group comparisons were performed using the Kruskal-Wallis test for continuous variables. Post-hoc analysis was conducted with the Wilcoxon-Mann-Whitney U test, corrected with Bonferroni adjustment for pairwise comparisons. The presence of age- and gender-adjusted differences was evaluated using the gtsummary R package. Statistical significance was set at $p < 0.05$.

A univariate ordinal regression was conducted with group membership (controls [CTRL], mild-moderate fibrosis [F1-F2], advanced fibrosis [F3-F4]) as the dependent variable and each ECM marker individually as the independent variable. The predicted probabilities of group membership were computed using the formula: $(Y \leq j) = \frac{1}{1+exp[-(\alpha_j - \beta X)]}$, where $P(Y \leq j)$ represents the cumulative probability of being in group j or lower, α_j is the threshold coefficient for the group j, β is the estimated coefficient for the predictor, and X is the observed value of the predictor. The probability of belonging to group j is then given by: $P(Y = j) = P(Y \leq j) - P(Y \leq j-1)$.

A stepwise selection approach based on the Bayesian Information Criterion (BIC) [26,27] was used to identify the most informative combination of markers to discriminate among the three classes. For this purpose, the dataset was split into a training set (66% of the data) and a test set (34% of the data). Model performance was evaluated on the test set by assessing the confusion matrix and calculating metrics such as accuracy, sensitivity, specificity, and negative predictive value, both overall and within each fibrosis group.

To further improve classification performance, we implemented an XGBoost model (eXtreme Gradient Boosting), a widely used machine learning algorithm known for its efficiency and ability to prevent overfitting in classification tasks. The model was used to classify patients into three categories: CTRL, F1-F2, and F3-F4. The XGBoost model was built and trained using a 5-fold cross-validation approach in Python.

The model was implemented by setting a reduced tree depth of 4 and a learning rate of 0.005 to allow for more gradual learning. Subsampling and column sampling rates were set at 0.8 to introduce randomness and prevent overfitting. Regularization techniques were applied, with L1 (lasso) and L2 (ridge) regularizations set at 1.0 and 2.0, respectively, to penalize complex models and further reduce overfitting.

The model's performance was evaluated through accuracy, sensitivity and specificity values for each fibrosis stage. To interpret the contribution of each variable to the model's predictions, SHAP (Shapley Additive Explanations) analysis was employed.

3. Results

3.1. Univariate and adjusted analysis of circulating markers across fibrosis stages

In Table 1, we present the demographic and laboratory characteristics of patients with mild-to-moderate fibrosis (F1-F2) and advanced fibrosis to cirrhosis (F3-F4), compared to healthy controls (CTRLs). Significant differences in gender distribution were observed, with a higher prevalence of males in the F3-F4 group. The median age increased progressively from controls to F1-F2 and F3-F4, reflecting disease progression in the pathological groups. Among the conventional markers, ALT, AST, GGT, and ALP levels showed progressive increases across the groups, while albumin and cholesterol levels decreased with increasing fibrosis severity in the pathological groups.

Table 1
Comparative analysis of demographic and laboratory parameters between mild-to-moderate fibrosis patients (F1-F2 METAVIR score) and advanced fibrosis to cirrhosis patients (F3-F4 METAVIR score). Parameters include gender distribution and median values with interquartile ranges (IQR) for various clinical measures. Statistical significance determined by Pearson's Chi-squared test for categorical variables and Wilcoxon rank sum test for continuous variables.

Characteristic	***CTRL, N = 30*[1]**	***F1-F2, N = 68*[1]**	***F3-F4, N = 66*[1]**	***p-value*[2]**
Sex				0.005
F	12 (40%)	45 (66%)	27 (41%)	
M	18 (60%)	23 (34%)	39 (59%)	
Age	58 (51, 64)	64 (58, 73)	72 (62, 79)	<0.001
ALT	14 (11, 18)	52 (36, 75)	76 (52, 137)	<0.001
AST	17 (15, 20)	43 (30, 67)	68 (44, 109)	<0.001
GGT	15 (11, 20)	58 (31, 80)	70 (47, 106)	<0.001
Albumin	4.18 (3.88, 4.47)	4.20 (4.00, 4.55)	4.00 (3.70, 4.20)	<0.001
ALP	57 (47, 68)	82 (67, 114)	103 (75, 120)	<0.001
Cholesterol	162 (141, 177)	181 (162, 200)	157 (141, 187)	<0.001
HB	14.0 (13.0, 15.0)	13.9 (13.3, 14.6)	13.9 (12.7, 15.0)	0.7
LN (range < 50 ng/mL)	10 (7, 12)	80 (61, 102)	118 (74, 221)	<0.001
CG (range < 2,7 µgr/mL)	0.7 (0.6, 1.0)	0.8 (0.5, 1.2)	3.8 (1.6, 11.5)	<0.001
C IV (range ≤30,0ng/mL)	16 (14, 17)	15 (12, 19)	69 (33, 100)	<0.001
HA (range ≤ 100ng/mL)	56 (50, 62)	65 (52, 72)	95 (74, 167)	<0.001
PIIIP N-P (range ≤ 30,0 ng/mL)	26 (24, 30)	260 (194, 321)	437 (310, 585)	<0.001
GP73 (range≤ 45 ng/ml)	21 (19, 23)	16 (10, 24)	32 (18, 45)	<0.001

1 n (%); Median (IQR).
2 Pearson's *Chi-squared test; Kruskal-Wallis rank sum test.*

Aside from conventional circulating markers, all ECM markers, including LN, HA, PIIIP N-P, and C-IV, together with emerging non-ECM markers such as CG and GP73, show statistically significant differences among the groups (Table 1). In Fig. 1, we present a more detailed breakdown of these differences, performing a post-hoc analysis with the Wilcoxon Mann-Whitney U Test and Bonferroni correction. This analysis reveals that HA, LN, and PIIIP N-P exhibit a gradual increase across the three groups (CTRL, F1-F2, F3-F4), with progressively higher values in each successive group. This difference is particularly pronounced for PIIIP N-P, which increases from 26 ng/mL in controls to 260 ng/mL in F1-F2 and 437 ng/mL in F3-F4.

For the remaining variables, including C-IV, CG, and GP73, a significant difference is observed between the two pathological groups ($p < 0.0001$), particularly remarkable in C-IV levels, which rise from 15 ng/mL in F1-F2 to 69 ng/mL in F3-F4. For these variables, the F1-F2 group more closely resembles the controls, with no statistically significant differences or without showing a monotonic increase across the three groups.

An analysis adjusted for sex and age was conducted to evaluate differences between groups, using F1-F2 as the reference group (Table 2). For the investigated markers, the adjusted results confirmed the patterns observed in Fig. 1. When comparing F3-F4 to F1-F2, significant adjusted increases were observed in all markers: C-IV (adjusted difference: 58.9 ng/mL, $p < 0.001$), CG (5.5 ng/mL, $p < 0.001$), GP73 (15.6 ng/mL, $p < 0.001$), HA (70.6 ng/mL, $p < 0.001$), LN (58.8 ng/mL, $p < 0.001$), and PIIIP N-P (163.9 ng/mL, $p < 0.001$). In the comparison between controls and the reference group, significant reductions were noted in LN (−66.5 ng/mL, $p < 0.001$) and PIIIP N-P (−250.1 ng/mL, $p < 0.001$), highlighting the lower levels of these markers in healthy individuals. However, no significant differences were found for C-IV or CG.

Overall, Table 2 reinforces the role of ECM markers as reliable indicators for differentiating fibrosis stages, particularly in distinguishing

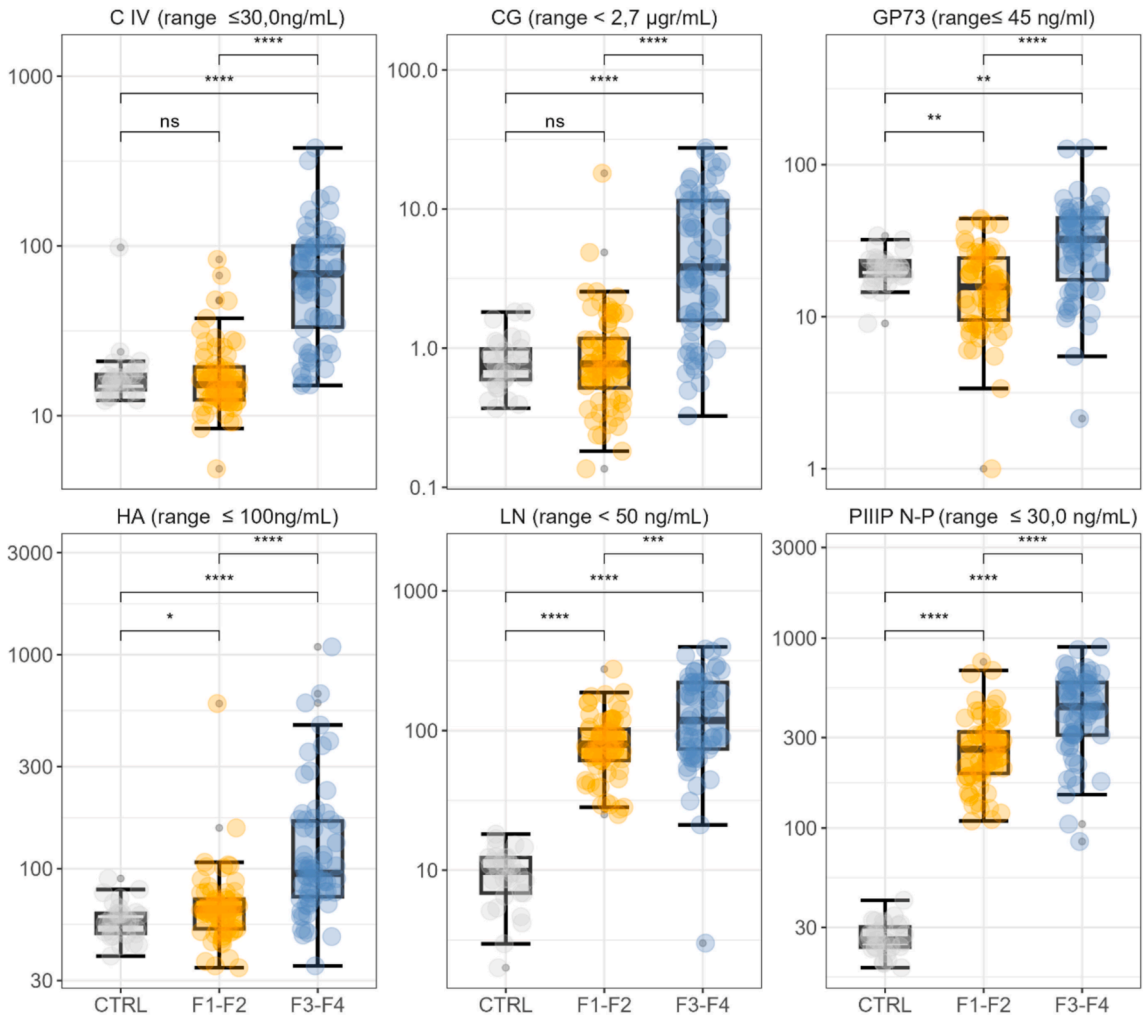

Fig. 1. Box plot analysis of selected extracellular matrix (ECM) components across three groups: healthy controls (CTRL), mild-to-moderate fibrosis (F1-F2), and advanced fibrosis to cirrhosis (F3-F4). The plots display the distribution of values for C-IV, HA, LN, and PIIIP N-P (ECM markers), along with emerging non-ECM markers CG and GP73. P-values from a post-hoc analysis (Wilcoxon rank sum test with Bonferroni correction) are included for each comparison.

Table 2
Adjusted differences for age and gender in laboratory parameters between healthy controls (CTRL), mild-to-moderate fibrosis (F1-F2 METAVIR score), and advanced fibrosis (F3-F4 METAVIR score), using F1-F2 as the reference group. The table reports adjusted differences, standard errors (SE), p-values, and 95% confidence intervals (CI) for each comparison.

	CTRL vs F1-F2				F3-F4 vs F1-F2			
OUTCOME	**Adj. Diff.**	**SE**	**p-value**	**95 % CI**	**Adj. Diff.**	**SE**	**p-value**	**95 % CI**
ALP	−33.41	7.68	2.58E-05	(−48.60, −18.23)	7.61	6.35	2.33E-01	(−4.94, 20.16)
ALT	−55.9	14.64	1.93E-04	(−84.82, −26.98)	21.32	11.6	6.80E-02	(−1.59, 44.23)
AST	−42.32	10.21	5.48E-05	(−62.47, −22.16)	19.03	8.07	1.96E-02	(3.09, 34.98)
ALBUMIN	−0.23	0.09	1.38E-02	(−0.40, −0.05)	−0.33	0.08	2.65E-05	(−0.48, −0.18)
CHOLESTEROL	−21.77	9.01	1.72E-02	(−39.60, −3.94)	−24.19	7.79	2.36E-03	(−39.61, −8.77)
GGT	−52.49	10.45	1.38E-06	(−73.12, −31.85)	14.24	8.34	8.95E-02	(−2.23, 30.71)
HB	−0.35	0.42	4.06E-01	(−1.18, 0.48)	−0.64	0.34	5.74E-02	(−1.31, 0.02)
C IV	2.55	9.89	7.97E-01	(−16.98, 22.08)	58.94	7.82	3.47E-12	(43.50, 74.39)
CG	−0.11	1.06	9.20E-01	(−2.21, 1.99)	5.54	0.84	6.32E-10	(3.88, 7.20)
GP73	5.56	3.65	1.29E-01	(−1.64, 12.77)	15.61	2.88	2.27E-07	(9.91, 21.31)
HA	0.91	26.37	9.73E-01	(−51.18, 53.00)	70.64	20.86	8.93E-04	(29.44, 111.84)
LN	−66.45	15.15	2.10E-05	(−96.37, −36.52)	58.82	11.98	2.27E-06	(35.15, 82.49)
PIIIP N-P	−250.12	33.11	3.12E-12	(−315.51, −184.73)	163.91	26.19	3.45E-09	(112.19, 215.63)

advanced from mild-to-moderate fibrosis.

3.2. Towards predictive Modelling of fibrosis stages based on Non-Invasive circulating markers with multivariate ordinal regression

Building on the differences observed in the previous section, we explored the potential utility of the investigated circulating markers for

classifying patients according to CLD stage. Given the ordered nature of the investigated categories, ordinal regression was used to model the probability of belonging to one of these three groups, with the stages of fibrosis progressing from controls to F1-F2, and finally to F3-F4.

The results of the ordinal regression analysis for ECM markers, together with CG and GP73 (Table 3), indicate that all models were highly significant, as reflected by the low p-values of the coefficients. Furthermore, the threshold coefficients between F1-F2 and F3-F4 were significant for all markers ($p < 0.05$), reinforcing the ability of these circulating markers to distinguish between mild-to-moderate and advanced stages of fibrosis. Similarly, the thresholds between controls and F1-F2 were significant for all markers, except for CG and GP73, where no significant differences were observed.

For completeness, Fig. 2 presents the predicted probability curves, based on the coefficients from Table 3, for classifying a patient into one of the three groups. A gradual shift in probabilities is observed for all markers, with PIIIP N-P (Panel F) showing a particularly sharp distinction.

To explore in greater detail the diagnostic potential of these markers, both individually and in combination, we conducted a multivariate ordinal regression analysis. For this purpose, the dataset was first split into a training set (66%) and a test set (34%). A stepwise ordinal regression using the Bayesian Information Criterion (BIC) was then applied to identify the most informative marker combination. This process led to the selection of PIIIP N-P, C-IV, and LN as the most informative combination of markers for classification. The selected model is summarized in Table 4.

The predicted probabilities of belonging to the three study groups were visualized in Fig. 3. The plots illustrate the probabilities for the control group (3A), F1-F2 (3B), and F3-F4 (3C), as a function of C-IV and PIIIP N-P levels, while holding LN constant at its median value. Based on the application of the model shown in panels 3A–C, we calculated the confusion matrix using the test set data, which is displayed in Fig. 3D. The confusion matrix reveals excellent classification of the CTRL (healthy) group versus the pathological groups, with minimal misclassifications. However, between the two pathological groups (F1-F2 and F3-F4), the model's classification is less precise, showing some overlap.

Following the evaluation of the confusion matrix, we calculated related performance metrics, which are reported in Table 4. The model demonstrates a moderate accuracy of 0.77 (95% CI: 0.60–0.90), reflecting reasonable overall classification performance. Sensitivity analysis shows strong performance for the CTRL group (0.90) and fairly high performance for the F1-F2 group (0.83), but sensitivity decreases for the F3-F4 group (0.62). In terms of specificity, the model performs perfectly for the CTRL group (1.0), with lower but still acceptable values for F1-F2 (0.78) and F3-F4 (0.86).

3.3. *Refining the prediction model with machine learning and explainable AI*

Although the multivariate ordinal regression produced statistically significant results, the sensitivity for the F3-F4 group (advanced fibrosis) remained relatively low, highlighting limitations in distinguishing more severe disease stages. To address this, we implemented an XGBoost classifier, which uses all the variables listed in Table 1. The choice of this algorithm is motivated by its ability to handle complex, non-linear patterns in the data while mitigating overfitting through mechanisms such as regularization (L1 and L2) and tree pruning. To increase the robustness of the model, we applied 5-fold cross-validation. The results of this cross-validation are summarized in Table 5, where we present performance metrics calculated by XGBoost for each fold, compared to the metrics from the previous ordinal regression model. XGBoost's results are expressed as the mean and 95% CI, calculated across the folds, and the same analysis is visualized graphically in Fig. 4A.

As shown in Fig. 4A, which compares the key performance metrics from XGBoost (bars) with those from the multivariate ordinal regression (blue dots), XGBoost exhibited improved performance across several metrics. The overall accuracy increased to 0.87 compared to 0.77 from the ordinal regression. Importantly, XGBoost enhanced sensitivity for the F3-F4 group, improving from 0.62 to 0.75, while maintaining strong sensitivity for the CTRL and F1-F2 groups. Specificity also remained high across all groups, with 1.0 for CTRL, 0.85 for F1-F2, and 0.87 for F3-F4, demonstrating the model's robustness. The XGBoost classifier not only improved sensitivity for advanced fibrosis stages but also maintained balanced performance across all groups, resolving the issue of misclassification seen between the F1-F2 and F3-F4 groups in the ordinal regression.

To identify the features that contributed most to the model's predictions, we applied SHAP analysis. Fig. 4B presents the SHAP results for a representative fold, where LN, PIIIP N-P, and C-IV rank among the top three features. For completeness, Fig. 5 displays the SHAP results across all folds, along with the average rankings, where these variables consistently rank highly, further underscoring their significance in fibrosis classification.

4. Discussion

Liver fibrosis is a pathological condition marked by an imbalance in the synthesis and degradation of the ECM within the liver, leading to excessive proliferation of mesenchymal cells. Triggers for this condition include viral infections, excessive alcohol intake, autoimmune diseases, and fatty acid accumulation in the liver [23,28]. As liver fibrosis progresses, it may evolve into cirrhosis, a more severe stage characterized by the liver's diminished capacity to compensate for damage. This loss of function leads to a range of complications that significantly degrade quality of life and impose economic burdens on families and society [29,30]. Given the chronic nature of liver fibrosis, early diagnosis and ongoing monitoring of its progression are critical for patient management [27,31–39].

In this study, we explored the role of circulating ECM-related markers, along with non-ECM emerging markers, in differentiating fibrosis stages across three distinct groups: CTRL, F1-F2, and F3-F4.

In terms of demographic parameters, our study highlights statistically significant differences in gender and age of participants among the three groups, necessitating the subsequent evaluation of age- and

Table 3
Results of the ordinal regression analysis for ECM markers (C-IV, PIIIP N-P, HA, LN), together with emerging non-ECM markers (CG, GP73), used for classifying patients across the three stages of chronic liver disease (CTRL, F1-F2, F3-F4). Coefficients (Estimates), standard errors (SE), and p-values are reported for each variable. Threshold coefficients between CTRL|F1-F2 and F1-F2|F3-F4 are included to indicate the significance of distinguishing between these stages of fibrosis. Asterisks denote statistical significance levels as follows: *$p < 0.05$, **$p < 0.01$, ***$p < 0.001$, and ****$p < 0.0001$.

VARIABLE	ESTIMATE	SE	P-VALUE	CTRL|F1-F2 ESTIMATE	CTRL|F1-F2 SE	F1-F2|F3-F4 ESTIMATE	F1-F2|F3-F4 SE
C-IV	0.072	0.0138	<0.000	0.8142*	0.3543	3.3221*	0.526
PIIIP N-P	0.014	0.002	<0.000	1.4937*	0.3933	4.8856*	0.6881
CG	1.1597	0.2875	<0.000	0.4867	0.3458	2.9628*	0.4972
GP73	0.0703	0.0157	<0.000	0.6198	0.4032	2.4006*	0.4636
HA	0.0643	0.0124	<0.000	3.4077*	0.8158	5.746*	0.9703
LN	0.0304	0.0048	<0.000	0.9427*	0.3444	3.6489*	0.5263

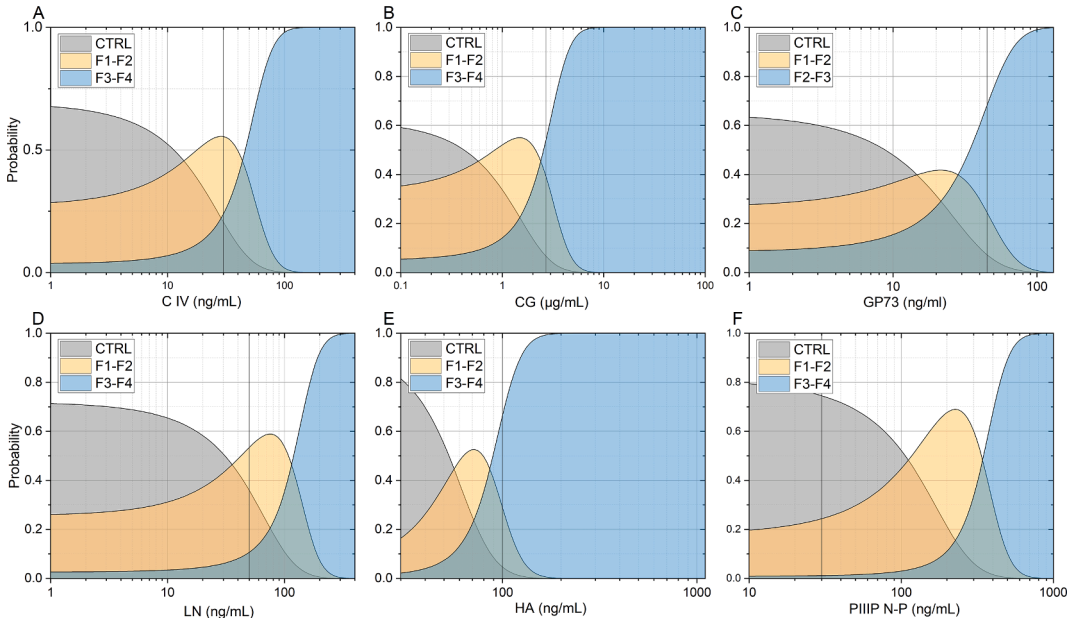

Fig. 2. Predicted probabilities of group membership (CTRL, F1-F2, F3-F4) for each circulating marker, based on the ordinal regression models. Each panel (A-F) corresponds to a different marker: (A) C-IV, (B) CG, (C) GP73, (D) LN, (E) HA, and (F) PIIIP N-P. The y-axis shows the predicted probability, while the x-axis displays the marker concentration in ng/mL or µg/mL. The shaded areas represent the probability distribution for belonging to one of the three groups: grey for healthy controls (CTRL), gold for mild-to-moderate fibrosis (F1-F2), and cyan for advanced fibrosis (F3-F4).

Table 4
Multivariate ordinal regression model selected through a stepwise procedure based on the BIC criterion, starting from a full model that included all parameters listed in Table 1. The model includes LN (range < 50 ng/mL), C IV (range ≤ 30.0 ng/mL), and PIIIP N-P (range ≤ 30.0 ng/mL) as independent variables, with thresholds defined between the CTRL, F1-F2, and F3-F4 groups. The coefficients for the variables and thresholds are reported along with their standard errors, z-values, and statistical significance levels. The model was developed using the training set, while performance metrics, including accuracy (0.77; 95 % CI: 0.60–0.90), sensitivity, and specificity, were obtained from the test set. Statistical significance levels are indicated as follows: ***p < 0.001, **p < 0.01, *p < 0.05.

Variable[1]/ Threshold[2]/metric[3]	dataset	Estimate	SE	Z-value	P-value
LN[1]	Training	0.013	0.011	1.19	0.233
C-IV[1]	Training	0.092	0.035	2.66	0.0078 **
PIIIP N-P[1]	Training	0.0084	0.0039	2.16	0.031 *
Threshold CTRL vs F1-F2[2]	Training	2.95	0.795	3.71	0.0002 ***
Threshold F1-F2 vs F3-F4[2]	Training	8.71	1.91	4.56	< 0.0001 ***
Accuracy[3]	Test	0.77. 95 % CI: (0.60, 0.90)			
Sensitivity[3]	Test	0.90(CTRL); 0.83(F1-F2); 0.62 (F3-F4)			
Specificity[3]	Test	1.0 (CTRL); 0.78 (F1-F2); 0.86 (F3-F4)			

gender-adjusted differences. Specifically, we observed a higher prevalence of males among patients with advanced fibrosis to cirrhosis, which aligns with the current literature [40]. However, it is important to note that numerous studies in recent years have demonstrated an increase in cirrhosis among women [41–43]. Additionally, we observed a significant increase in age across the groups, consistent with disease development and evolution.

The progression of fibrosis is typically associated with significant changes in liver architecture and function, with ECM markers reflecting these structural changes [44–46]. Accordingly, our univariate (Table 1) and age- and gender-adjusted (Table 2) analyses revealed remarkable changes in the levels of all ECM components across groups. Notably, C-IV levels showed a marked increase between the mild (F1-F2) and advanced (F3-F4) stages, corroborating its established role in liver fibrosis. This is in perfect agreement with previous findings that demonstrated C-IV's effective discrimination between early and advanced fibrosis stages, with significant elevations in stages ≥F3 compared to F0-F2 ($p<0.05$) [47]. Similarly, Dong et al. observed in HBV patients that C-IV had the highest correlation with disease severity (Spearman's rho = 0.538), reinforcing its reliability as a fibrosis staging marker [48]. Indeed, collagen type IV, located in the basement membrane, supports hepatocytes and facilitates the bidirectional flow of nutrients and metabolites. In a healthy liver, its production is primarily managed by the sinusoidal endothelium and biliary epithelium, but during liver damage, portal fibroblasts and hepatic stellate cells also contribute, emphasizing its crucial role in the liver's response to injury [49,50].

PIIIP N-P also emerged as a strong biomarker candidate, with its gradual increase in concentration from healthy controls to patients with advanced fibrosis. In this regard, previous studies in the literature have highlighted its association with the severity of liver fibrosis, as evidenced in various clinical scenarios. Rio et al. explored the use of PIIIP N-P as a marker for early detection of veno-occlusive disease after bone marrow transplantation, highlighting its role in monitoring hepatic fibrosis [51]. Walsh et al. analyzed PIIIP N-P in chronic HCV, demonstrating its utility in assessing liver disease severity through assays measuring collagen dynamics [52]. Additionally, extensive research has explored the combined use of multiple markers for liver staging, such as Guechot et al.'s work combining PIIIP N-P and HA to stage liver fibrosis in chronic HCV patients [53].

In line with previous research, we conducted a multivariate analysis to assess the effectiveness of combining circulating and demographic markers for CLD staging. A stepwise multivariate ordinal regression identified LN, C-IV, and PIIIP N-P as the most informative markers for classifying patients across the three fibrosis stages. While the model showed good specificity and accuracy, its sensitivity for the F3-F4 group remained suboptimal (Fig. 5), indicating the need for alternative approaches to improve staging accuracy.

In this context, Hoffman et al. have recently highlighted the transformative role that machine learning is playing in laboratory medicine, emphasizing its ability to enhance diagnostic and predictive capabilities in complex medical environments [54]. XGBoost, in particular, stands

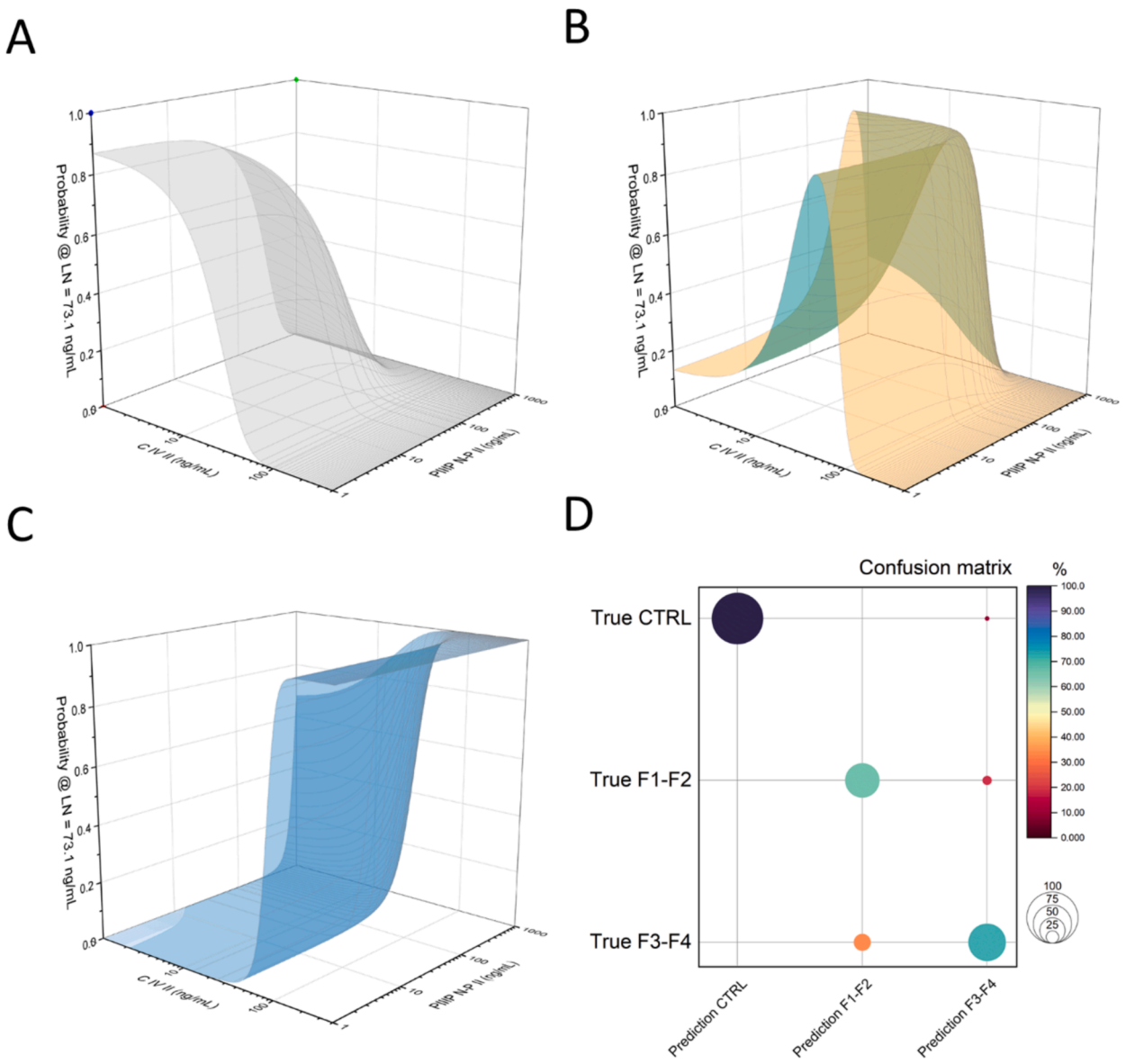

Fig. 3. Probability surface plots illustrating the likelihood for a patient to belong to the control group (A), F1-F2 group (B), and F3-F4 group (C) as a function of C-IV and PIIIP levels. The surfaces are shown while keeping LN constant at its median value. Panel (D) presents the confusion matrix obtained by evaluating the selected model on the training set.

Table 5
Performance metrics comparison between the XGBoost classifier and multivariate ordinal regression for liver fibrosis staging. The XGBoost model was implemented with 5-fold cross-validation, and its results are presented as the mean and 95% confidence interval (CI) across folds.

MODEL	ACCURACY	SENSITIVITY (CTRL)	SENSITIVITY (F1-F2)	SENSITIVITY (F3-F4)	SPECIFICITY (CTRL)	SPECIFICITY (F1-F2)	SPECIFICITY (F3-F4)
XGBOOST FOLD 1	0.79	1	0.73	0.71	1	0.82	0.84
XGBOOST FOLD 2	0.88	1	0.82	0.89	1	0.94	0.88
XGBOOST FOLD 3	0.91	1	0.92	0.87	1	0.9	0.94
XGBOOST FOLD 4	0.88	1	1	0.69	1	0.79	1
XGBOOST FOLD 5	0.88	1	0.85	0.87	0.96	0.95	0.88
AVERAGE (95 % CI)	0.87 (0.81–0.93)	1.00 (1.00–1.00)	0.86 (0.74–0.99)	0.81 (0.69–0.93)	0.99 (0.97–1.0)	0.88 (0.79–0.97)	0.91 (0.83–0.99)
ORDINAL REGRESSION	0.77	0.9	0.83	0.62	1	0.78	0.86

out among machine learning methods for its effectiveness in medical applications. Its advanced features, such as the combination of weak learners, tree pruning, and regularization techniques, help prevent overfitting [55,56]. For instance, Li et al. demonstrated how XGBoost could identify gene signatures to predict metastatic status in breast cancer, showcasing its superior performance compared to traditional classifiers [57]. Additionally, the integration of XGBoost with Explainable Artificial Intelligence (XAI) techniques, such as SHAP, has shown

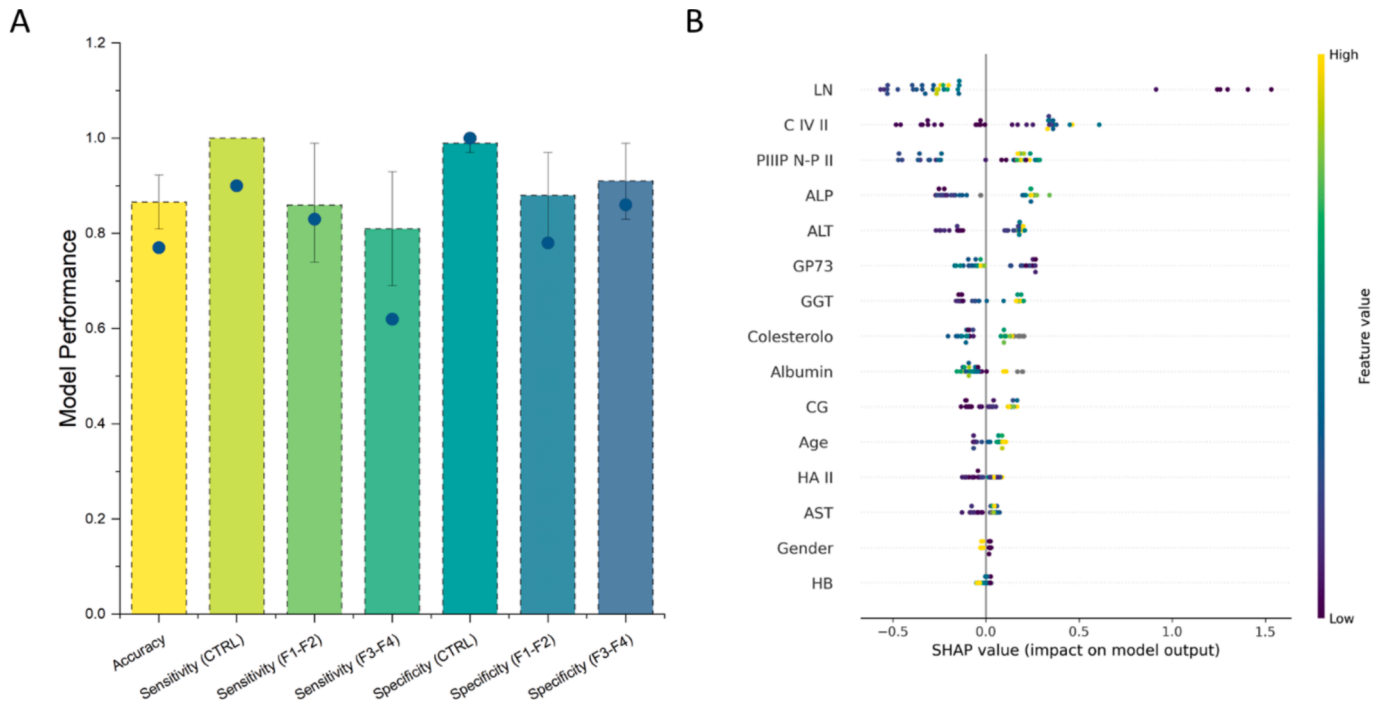

Fig. 4. (A) Comparison of key performance metrics between XGBoost (bars) and multivariate ordinal regression (blue dots). The bars represent XGBoost results expressed as mean values with 95% confidence intervals calculated across 5-fold cross-validation. Metrics include accuracy, sensitivity and specificity for the control group (CTRL), F1-F2, and F3-F4 groups. The blue dots represent the corresponding values from the multivariate ordinal regression model. (B) Representative SHAP summary plot for one of the cross-validation folds, showing the overall contribution of each feature to the model's predictions across all three classes (CTRL, F1-F2, F3-F4). The x-axis shows the SHAP values, representing the impact of each feature on the model's output. Positive SHAP values indicate that the feature pushes the prediction towards higher fibrosis stages (F1-F2, F3-F4), while negative SHAP values push it towards the control group (CTRL). The colors represent the feature values, with yellow indicating high values and purple indicating low values.

great promise. SHAP, a key XAI tool, highlights the features that most significantly impact model predictions, providing clinicians with clear, transparent, and actionable insights [58]. Yi et al. employed the combination of XGBoost and SHAP to handle complex, imbalanced data in Alzheimer's diagnostics, with SHAP providing insights into the factors driving predictions [57]. Similarly, Zelli et al. fine-tuned model parameters and applied SHAP to better understand how demographic and clinical features contribute to predicting Alzheimer's disease progression [59].

Our study aligns with the above-mentioned recent advancements by implementing a 5-fold cross-validated XGBoost model, which significantly outperformed the ordinal regression models, particularly in severe pathological cases (Table 5). The model achieved an overall accuracy of 0.87, compared to 0.77 for the ordinal regression, with sensitivity for the F3-F4 group improving from 0.62 to 0.75. Specificity remained consistently high across all groups, nearing 1.0 for the control group, with balanced performance across pathological stages.

To further understand the model's predictions, we employed SHAP across all folds, which consistently highlighted LN, C-IV, and PIIIP N-P as the most influential features driving the model's output (Fig. 5). Notably, these are the same variables selected by the stepwise regression approach, further reinforcing the robustness and importance of these markers across different modeling methodologies. This consistency between machine learning and traditional statistical methods strengthens the reliability of these markers for fibrosis staging.

5. Conclusion

In conclusion, the results of this study demonstrate the significant potential of ECM-related biomarkers in non-invasive staging of CLD, especially among HCV-positive patients. The notable increase in ECM components (HA, LN, PIIIP N-P, and C-IV), along with emerging non-ECM markers (CG and GP73), in patients with advanced fibrosis underscores their utility in reflecting the severity of liver fibrosis. Particularly, the combination of C-IV, PIIIP N-P, and LN emerged as the most diagnostically relevant markers, offering robust performance in distinguishing between mild, moderate, and advanced fibrosis stages.

Furthermore, this study provides preliminary evidence supporting the application of advanced machine learning techniques like XGBoost to enhance diagnostic accuracy. The XGBoost model demonstrated superior classification performance compared to traditional regression models, likely due to its ability to process a larger number of variables simultaneously, while avoiding overfitting through regularization techniques. This allows for more reliable predictions on the test set, maintaining high accuracy across all fibrosis stages.

The use of XAI tools such as SHAP further highlights the clinical value of this approach, offering transparency in model predictions. SHAP's ability to identify key variables such as LN, C-IV, and PIIIP N-P in the decision-making process supports their role as pivotal markers for fibrosis staging, and provides clinicians with clear insights that could guide more personalized treatment decisions.

Our findings suggest that combining traditional fibrosis biomarkers with modern machine learning approaches could significantly improve non-invasive fibrosis staging. The consistent ranking of LN, C-IV, and PIIIP N-P across both statistical and machine learning models reinforces their importance as key indicators of fibrosis progression. Future studies should focus on validating these results in larger patient cohorts and exploring the integration of ECM markers into multi-marker panels, aimed at improving the non-invasive diagnosis and monitoring of CLD.

6. Institutional Review Board Statement

The study was conducted in accordance with the Declaration of Helsinki guidelines and received approval from the Regional Ethical

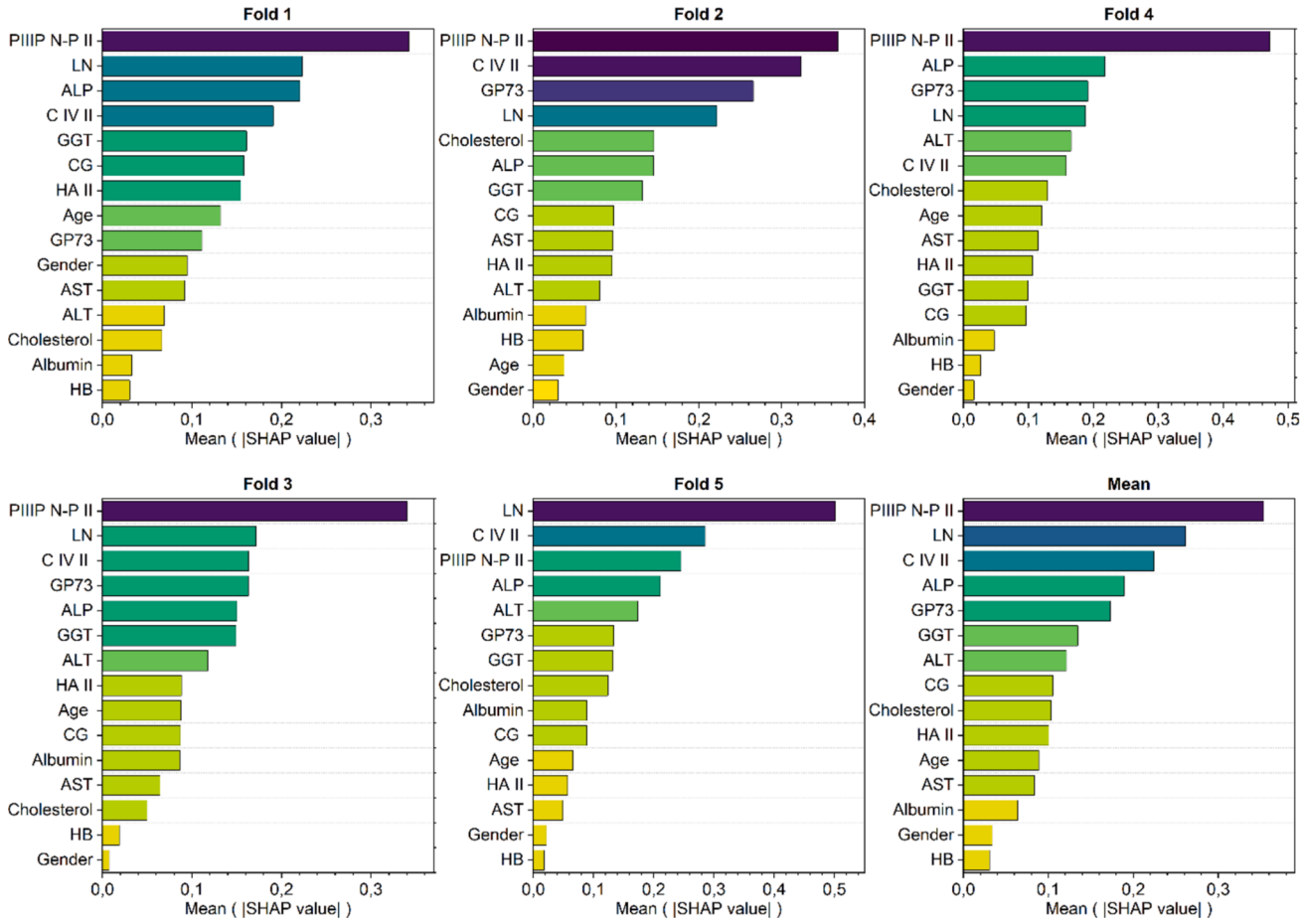

Fig. 5. SHAP (Shapley Additive Explanations) results across all folds, along with the mean SHAP values among folds. Laminin, PIIIP N-P, and collagen-IV consistently rank among the top features, with their average contributions among folds further highlighting their importance in fibrosis classification.

Committee for Clinical Experimentation of the Tuscany Region, acting as the ethics committee for the University of Florence (Approval No. 12924).

Informed Consent Statement

All participants provided written informed consent.

CRediT authorship contribution statement

Valeria Carnazzo: Writing – original draft, Methodology, Conceptualization. **Stefano Pignalosa:** Writing – original draft. **Marzia Tagliaferro:** Writing – original draft. **Laura Gragnani:** Conceptualization. **Anna Linda Zignego:** Conceptualization. **Cosimo Racco:** Writing – original draft. **Luigi Di Biase:** Methodology. **Valerio Basile:** Investigation. **Gian Ludovico Rapaccini:** Investigation. **Riccardo Di Santo:** Data curation. **Benedetta Niccolini:** Data curation. **Mariapaola Marino:** Writing – review & editing, Funding acquisition. **Marco De Spirito:** Data curation. **Guido Gigante:** Data curation. **Gabriele Ciasca:** Data Analysis, Writing, Review & Editing. **Umberto Basile:** Writing – original draft, Supervision, Conceptualization.

Funding

This research and its publication have been funded from Università Cattolica del Sacro Cuore Fondazione Policlinico Universitario "A. Gemelli" IRCCS as a part of its programs on promotion and dissemination of scientific research (Linea D1 to M.M.) that we gratefully acknowledged.

Acknowledgments

All authors thank the The Data Analysis and visualization unit of Società Italiana di Biochimica Clinica e Biologia Molecolare Clinica - Medicina di Laboratorio regionale (Sibioc Lazio). Riccardo Di Santo was supported by Fondazione Umberto Veronesi, which is gratefully acknowledged.

References

[1] S. De Siervi, S. Cannito, C. Turato, Chronic liver disease: latest research in pathogenesis, detection and treatment, Int. J. Mol. Sci. 24 (2023) 10633.
[2] S. Cheemerla, M. Balakrishnan, Global epidemiology of chronic liver disease, Clin. Liver Dis. 17 (2021) 365–370.
[3] M. Parola, M. Pinzani, Liver fibrosis: Pathophysiology, pathogenetic targets and clinical issues, Mol. Aspects Med. 65 (2019) 37–55.
[4] N. Roehlen, E. Crouchet, T.F. Baumert, Liver fibrosis: mechanistic concepts and therapeutic perspectives, Cells 9 (2020) 875.
[5] G. Tong, X. Chen, J. Lee, J. Fan, S. Li, K. Zhu, et al., Fibroblast growth factor 18 attenuates liver fibrosis and HSCs activation via the SMO-LATS1-YAP pathway, Pharmacol. Res. 178 (2022) 106139.
[6] T. Kisseleva, D. Brenner, Molecular and cellular mechanisms of liver fibrosis and its regression, Nat. Rev. Gastroenterol. Hepatol. 18 (2021) 151–166.
[7] D. Schuppan, R. Surabattula, X.Y. Wang, Determinants of fibrosis progression and regression in NASH, J. Hepatol. 68 (2018) 238–250.
[8] Y. Lurie, M. Webb, R. Cytter-Kuint, S. Shteingart, G.Z. Lederkremer, Non-invasive diagnosis of liver fibrosis and cirrhosis, World J. Gastroenterol. 21 (2015) 11567.
[9] C. Li, R. Li, W. Zhang, Progress in non-invasive detection of liver fibrosis, CancerBiol Med 15 (2018) 124.
[10] R. Chou, N. Wasson, Blood tests to diagnose fibrosis or cirrhosis in patients with chronic hepatitis C virus infection: a systematic review, Ann. Intern. Med. 158 (2013) 807–820.
[11] L. Miele, T. De Michele, G. Marrone, M.A. Isgrò, U. Basile, C. Cefalo, et al., Enhanced liver fibrosis test as a reliable tool for assessing fibrosis in nonalcoholic fatty liver disease in a clinical setting, Int. J. Biol. Markers 32 (2017) 397–402.

[12] L.C. Bertot, G.P. Jeffrey, B. de Boer, Z. Wang, Y. Huang, G. Garas, et al., Comparative accuracy of clinical fibrosis markers, Hepascore and Fibroscan® to detect advanced fibrosis in patients with nonalcoholic fatty liver disease, DigDis. Sci 68 (2023) 2757–2767.
[13] B. Cylwik, A. Bauer, E. Gruszewska, K. Gan, M. Kazberuk, L. Chrostek, The Diagnostic value of FibroTest and hepascore as non-invasive markers of liver fibrosis in primary sclerosing cholangitis (PSC), J. Clin. Med. 12 (2023) 7552.
[14] G. Aleknavičiūtė-Valienė, V. Banys, Clinical importance of laboratory biomarkers in liver fibrosis, Biochem.. Medica 32 (2022) 346–356.
[15] N. Plevris, R. Sinha, A.W. Hay, N. McDonald, J.N. Plevris, P.C. Hayes, Index serum hyaluronic acid independently and accurately predicts mortality in patients with liver disease, Aliment Pharmacol Ther 48 (2018) 423–430.
[16] Y. Chen, G. Cai, C. Zhang, J. Yao, Z. Wang, Z. Wang, et al., The association of serum markers of fibrosis and development of liver cirrhosis in chronic hepatitis B patients: a systematic review and meta-analysis, Cogent Med. 6 (2019) 1619896.
[17] K.M. Mak, R. Mei, Basement membrane type IV collagen and laminin: an overview of their biology and value as fibrosis biomarkers of liver disease, Anat Rec 300 (2017) 1371–1390.
[18] J.B. Larsen, C.S. Knudsen, T. Parkner, Procollagen III, N-terminal propeptide (PIIINP): establishment of reference intervals in Northern European adults and children using the MAGLUMI 800 chemiluminescence immunoassay, Scand J Clin Lab Invest 81 (2021) 389–393.
[19] M. Gudowska, E. Gruszewska, A. Panasiuk, B. Cylwik, M. Swiderska, R. Flisiak, et al., High serum N-terminal propeptide of procollagen type III concentration is associated with liver diseases, Gastroenterol Rev Gastroenterol 12 (2017) 203–207.
[20] J.T. Stefano, L.V. Guedes, A.A.A. de Souza, D.S. Vanni, V.A.F. Alves, F.J. Carrilho, et al., Usefulness of collagen type IV in the detection of significant liver fibrosis in nonalcoholic fatty liver disease, Ann Hepatol 20 (2021) 100253.
[21] T. Okanoue, H. Ebise, T. Kai, M. Mizuno, T. Shima, J. Ichihara, et al., A simple scoring system using type IV collagen 7S and aspartate aminotransferase for diagnosing nonalcoholic steatohepatitis and related fibrosis, J Gastroenterol 53 (2018) 129–139.
[22] G. Antonelli, S. Visentin, A. Tasinato, G. Rocco, F. Zemin, E. Volentier, et al., Cholylglycine determination by an automated chemiluminescence immunoassay: preliminary results in the intrahepatic cholestasis of pregnancy, J Lab Precis Med 4 (2019).
[23] S.L. Friedman, M. Pinzani, Hepatic fibrosis 2022: Unmet needs and a blueprint for the future, Hepatology 75 (2022) 473–488.
[24] N.K. Gatselis, T. Tornai, Z. Shums, K. Zachou, A. Saitis, S. Gabeta, et al., Golgi protein-73: A biomarker for assessing cirrhosis and prognosis of liver disease patients, World J Gastroenterol 26 (2020) 5130.
[25] Sjoberg DD, Whiting K, Curry M, Lavery JA, Larmarange J. Reproducible Summary Tables with the gtsummary Package. R J 2021;13.
[26] C. Napodano, C. Callà, A. Fiorita, M. Marino, E. Taddei, T. Di Cesare, et al., Salivary Biomarkers in COVID-19 Patients: Towards a Wide-Scale Test for Monitoring Disease Activity, J Pers Med 11 (2021) 385.
[27] R. Di Santo, M. Vaccaro, S. Romanò, F. Di Giacinto, M. Papi, G.L. Rapaccini, et al., Machine Learning-Assisted FTIR Analysis of Circulating Extracellular Vesicles for Cancer Liquid Biopsy, J Pers Med 12 (2022) 949.
[28] R.M. Dawood, M.A. El-Meguid, G.M. Salum, M.K. El Awady, Key players of hepatic fibrosis, J Interf Cytokine Res 40 (2020) 472–489.
[29] K. Weissenborn, Hepatic encephalopathy: definition, clinical grading and diagnostic principles, Drugs 79 (2019) 5–9.
[30] N. Elleuch, S. Mrabet, B. Slama, H. Jaziri, A. Hammami, A. Brahim, et al., Cirrhotic cardiomyopathy, Tunis. Med. 98 (2020) 206–210.
[31] G. Gheorghe, S. Bungău, G. Ceobanu, M. Ilie, N. Bacalbaşa, O.G. Bratu, et al., The non-invasive assessment of hepatic fibrosis, J Formos Med Assoc 120 (2021) 794–803.
[32] K. Pocino, A. Stefanile, V. Basile, C. Napodano, F. D'Ambrosio, R. Di Santo, et al., Cytokines and hepatocellular carcinoma: biomarkers of a deadly embrace, J Pers Med 13 (2022) 5.
[33] K. Pocino, C. Napodano, M. Marino, R. Di Santo, L. Miele, N. De Matthaeis, et al., A comparative study of serum angiogenic biomarkers in cirrhosis and hepatocellular carcinoma, Cancers (Basel) 14 (2021) 11.
[34] M. Leo, F. Di Giacinto, M. Nardini, A. Mazzini, C. Rossi, E. Porceddu, et al., Erythrocyte viscoelastic recovery after liver transplantation in a cirrhotic patient affected by spur cell anaemia, J Microsc (2020), https://doi.org/10.1111/jmi.12958.
[35] K. Pocino, C. Napodano, L. Gragnani, G. Ciasca, S. Colantuono, S. Marri, et al., Revealed the mystery of HBV related mixed cryoglobulinemia: potential biomarkers of disease progression, Rheumatology (Oxford) (2021).
[36] C. Napodano, G. Ciasca, P. Chiusolo, K. Pocino, L. Gragnani, A. Stefanile, et al., Serological and molecular characterization of hepatitis C virus-related cryoglobulinemic vasculitis in patients without cryoprecipitate, Int J Mol Sci 24 (2023) 11602.
[37] U. Basile, L. Miele, C. Napodano, G. Ciasca, F. Gulli, K. Pocino, et al., The diagnostic performance of PIVKA-II in metabolic and viral hepatocellular carcinoma: a pilot study, Eur Rev Med Pharmacol Sci 24 (2020) 12675–12685.
[38] R. Di Santo, F. Verdelli, B. Niccolini, S. Varca, A. Del Gaudio, F. Di Giacinto, et al., Exploring novel circulating biomarkers for liver cancer through extracellular vesicle characterization with infrared spectroscopy and plasmonics, Anal Chim Acta 1319 (2024) 342959.
[39] M. Tagliaferro, M. Marino, V. Basile, K. Pocino, G.L. Rapaccini, G. Ciasca, et al., New biomarkers in liver fibrosis: a pass through the quicksand? J Pers Med 14 (2024) 798.
[40] Y.-B. Liu, M.-K. Chen, Epidemiology of liver cirrhosis and associated complications: current knowledge and future directions, World J Gastroenterol 28 (2022) 5910.
[41] E.B. Tapper, N.D. Parikh, Diagnosis and management of cirrhosis and its complications: a review, J. Am. Med. Assoc. 329 (2023) 1589–1602.
[42] J.A. Flemming, Y. Dewit, J.M. Mah, J. Saperia, P.A. Groome, C.M. Booth, Incidence of cirrhosis in young birth cohorts in Canada from 1997 to 2016: a retrospective population-based study, LancetGastroenterol Hepatol 4 (2019) 217–226.
[43] D. Bizzaro, C. Becchetti, S. Trapani, B. Lavezzo, A. Zanetto, F. D'Arcangelo, et al., Influence of sex in alcohol-related liver disease: pre-clinical and clinical settings, United Eur Gastroenterol J 11 (2023) 218–227.
[44] Y. Vali, J. Lee, J. Boursier, R. Spijker, J. Verheij, M.J. Brosnan, et al., FibroTest for evaluating fibrosis in non-alcoholic fatty liver disease patients: a systematic review and meta-analysis, J Clin Med 10 (2021) 2415.
[45] W. He, C. Dai, Key Fibrogenic signaling, Curr Pathobiol Rep 3 (2015) 183–192.
[46] C.E. McQuitty, R. Williams, S. Chokshi, L. Urbani, Immunomodulatory role of the extracellular matrix within the liver disease microenvironment, Front Immunol 11 (2020) 574276.
[47] M.J. Nielsen, K. Kazankov, D.J. Leeming, M.A. Karsdal, A. Krag, F. Barrera, et al., Markers of collagen remodeling detect clinically significant fibrosis in chronic hepatitis C patients, PLoS One 10 (2015) e0137302.
[48] H. Dong, C. Xu, W. Zhou, Y. Liao, J. Cao, Z. Li, et al., The combination of 5 serum markers compared to FibroScan to predict significant liver fibrosis in patients with chronic hepatitis B virus, Clin Chim Acta 483 (2018) 145–150.
[49] M.A. Karsdal, S.H. Nielsen, D.J. Leeming, L.L. Langholm, M.J. Nielsen, T. Manon-Jensen, et al., The good and the bad collagens of fibrosis–their role in signaling and organ function, Adv Drug Deliv Rev 121 (2017) 43–56.
[50] M.A. Karsdal, S.T. Hjuler, Y.I. Luo, D.G.K. Rasmussen, M.J. Nielsen, S. Holm Nielsen, et al., Assessment of liver fibrosis progression and regression by a serological collagen turnover profile, Am J Physiol Liver Physiol 316 (2019) G25–G31.
[51] B. Rio, F. Bauduer, J.P. Arrago, R. Zittoun, N-terminal peptide of type III procollagen: A marker for the development of hepatic veno-occlusive disease after BMT and a basis for determining the timing of prophylactic heparin, Bone Marrow Transplant. 11 (1993) 471–472.
[52] K.M. Walsh, A. Fletcher, R.N.M. MacSween, A.J. Morris, Comparison of assays for N-amino terminal propeptide of type III procollagen in chronic hepatitis C by using receiver operating characteristic analysis, Eur J Gastroenterol Hepatol 11 (1999) 827–832.
[53] J. Guechot, A. Laudat, A. Loria, L. Serfaty, R. Poupon, J. Giboudeau, Diagnostic accuracy of hyaluronan and type III procollagen amino-terminal peptide serum assays as markers of liver fibrosis in chronic viral hepatitis C evaluated by ROC curve analysis, Clin Chem 42 (1996) 558–563.
[54] G. Hoffmann, F. Klawonn, At the crossroads between statistics and artificial intelligence: statistical learning in laboratory medicine, J Lab Med (2024).
[55] Nielsen D. Tree boosting with xgboost-why does xgboost win" every" machine learning competition? 2016.
[56] T. Chen, G.C. Xgboost, A scalable tree boosting system. Proc. 22nd acm sigkdd Int, Conf. Knowl. Discov. Data Min. (2016) 785–794.
[57] F. Yi, H. Yang, D. Chen, Y. Qin, H. Han, J. Cui, et al., XGBoost-SHAP-based interpretable diagnostic framework for alzheimer's disease, BMC Med Inform Decis Mak 23 (2023) 137.
[58] S.M. Lundberg, G.G. Erion, S.-I. Lee, Consistent individualized feature attribution for tree ensembles, ArXiv Prepr ArXiv180203888 (2018).
[59] V. Zelli, A. Manno, C. Compagnoni, R.O. Ibraheem, F. Zazzeroni, E. Alesse, et al., Classification of tumor types using XGBoost machine learning model: a vector space transformation of genomic alterations, J Transl Med 21 (2023) 836.